学位論文

SIRT7 regulates lipogenesis in adipocytes through deacetylation of PPARγ2

（SIRT7 は PPARγ2 の脱アセチル化を介して脂質合成を制御する）

ファテマ　アクター
AKTER FATEMA

Academic advisor

Professor Kazuya Yamagata
Department of Medical Biochemistry, Medical Sciences Major,
Doctoral Course of the Graduate School of Medical Sciences,
Kumamoto University

AY2021

学位論文

Title of Thesis : **SIRT7 regulates lipogenesis in adipocytes through deacetylation of PPARγ2**
（SIRT7 は PPARγ2 の脱アセチル化を介して脂質合成を制御する）

Name of Author : **AKTER Fatema**

Name of supervisor : Professor **YAMAGATA Kazuya**
Department of Medical Biochemistry, Medical Sciences Major, Doctoral Course of the Graduate School of Medical Sciences

Name of examiner : Professor **ARAKI Eiichi** Department of Metabolic Medicine

Professor **OIKE Yuichi** Department of Molecular Genetics

Professor **SAWA Tomohiro** Department of Microbiology

Professor **HINO Shinjiro** Department of Medical Cell Biology

AY 2021

SIRT7 regulates lipogenesis in adipocytes through deacetylation of PPARγ2

Fatema Akter[1], Tomonori Tsuyama[2], Tatsuya Yoshizawa[1], Shihab U. Sobuz[1], Kazuya Yamagata[1,2]

[1]Department of Medical Biochemistry, Faculty of Life Sciences, Kumamoto University, Kumamoto 860-8556, Japan

[2]Center for Metabolic Regulation of Healthy Aging (CMHA), Faculty of Life Sciences, Kumamoto University, Kumamoto 860-8556, Japan

Running title: SIRT7 deacetylates PPARγ2

Correspondence to:

Tatsuya Yoshizawa, PhD

Department of Medical Biochemistry,

Faculty of Life Sciences,

Kumamoto University

1-1-1 Honjo, Kumamoto,

Kumamoto 860-8556, Japan

Tel: +81-96-373-5070

Fax: +81-96-364-6940

e-mail: yoshizaw@kumamoto-u.ac.jp

Abstract

Aims/Introduction

Peroxisome proliferator-activated receptor (PPAR)-γ2 is a transcription factor crucial for regulating adipogenesis and glucose/lipid metabolism, and synthetic PPARγ ligands, such as thiazolidinediones, are effective oral medication for type 2 diabetes. Sirtuin 7 (SIRT7), a nicotinamide adenine dinucleotide-dependent deacetylase, also controls metabolism. However, it is not known whether SIRT7 regulates the function of PPARγ2 by its deacetylation.

Materials and Methods

Physical interaction between SIRT7 and PPARγ2, the effect of SIRT7 on PPARγ2 acetylation, and the deacetylation residue targeted by SIRT7 were investigated. The effects of PPARγ2 K382 acetylation on lipid accumulation, gene expression in C3H10T1/2 cell-derived adipocytes, and ligand-dependent transactivation activity were also evaluated.

Results

We demonstrated that SIRT7 binds to PPARγ2 and deacetylates PPARγ2 at K382. C3H10T1/2-derived adipocytes expressing PPARγ2^{K382Q} (a mimic of acetylated K) accumulated much less fat than adipocytes expressing wild-type PPARγ2 or PPARγ2^{K382R} (a mimic of nonacetylated K). Global gene expression analysis of adipocytes expressing PPARγ2^{K382Q} revealed that K382Q caused the dysregulation of a set of genes involved in lipogenesis, including *Srebp1c, Acaca*, *Fasn*, and *Scd1*. The rosiglitazone-dependent transcriptional activity of PPARγ2^{K382Q} was reduced compared with that of PPARγ2^{K382R}.

Conclusion

Our findings indicate that SIRT7-dependent PPARγ2 deacetylation at K382 controls lipogenesis in adipocytes.

Keywords

SIRT7, PPARγ, Acetylation, Lipogenesis

Introduction

Peroxisome proliferator-activated receptor (PPAR)-γ is a transcription factor belonging to the nuclear receptor superfamily. Similar to other nuclear receptors, PPARγ has several functional domains, including an N-terminal transactivation domain, a DNA-binding domain (DBD), and a C-terminal region that forms a ligand-binding domain (LBD), which has a ligand-dependent transactivation function. PPARγ binds to PPAR response elements (PPRE) with the retinoid X receptor to regulate the expression of various genes involved in adipogenesis, lipid metabolism, and insulin sensitivity [1, 2]. PPARγ has two isoforms: PPARγ1 and PPARγ2. Whereas PPARγ1 is expressed in many tissues, PPARγ2 is selectively expressed at high levels in white adipose tissue (WAT). Endogenous ligands for PPARγ include unsaturated fatty acids and 15-deoxy-prostaglandin J2 [3]. Ligand binding induces a conformational change in the receptor that allows for the differential recruitment of cofactors and subsequent modulation of PPARγ activity [1]. Synthetic PPARγ ligands (thiazolidinediones) are effective insulin sensitizers and they improve hyperinsulinemia and hyperglycemia in patients with type 2 diabetes [4]. The transcriptional activity of PPARγ is also regulated by post-translational modifications, including phosphorylation, acetylation, and SUMOylation [1, 4].

Sirtuins (SIRT1–7 in mammals) are evolutionarily conserved nicotinamide adenine dinucleotide-dependent deacetylases/deacylases that regulate a large number of biological processes, including metabolism [5, 6]. SIRT1 inhibits adipogenesis and enhances lipid mobilization from white adipocytes through the suppression of PPARγ activity by docking with nuclear receptor co-repressor [7]. SIRT1 also promotes adipocyte browning through deacetylation of PPARγ2 at K268 and K293 [8]. Although the physiological roles of SIRT7 are poorly defined, recent studies have revealed that it performs various roles in metabolism by deacetylating target proteins [9-12]. Fang *et al*. reported that SIRT7 promotes adipogenesis by inhibiting the autocatalytic activation of SIRT1 [13], indicating that SIRT7 indirectly regulates PPARγ activity. However, it is not known whether SIRT7 directly regulates PPARγ activity through its deacetylation.

In this report, we demonstrated that SIRT7 interacts with the LBD of PPARγ2 and deacetylates PPARγ2 at K382. Mouse mesenchymal C3H10T1/2 cell-derived adipocytes expressing PPARγ2^{K382Q} accumulated much less fat than adipocytes expressing wild-type (WT) PPARγ2 or PPARγ2^{K382R}. Global gene expression analysis of adipocytes expressing PPARγ2^{K382Q} revealed that K382Q caused the dysregulation of a set of genes involved in lipogenesis, including *Srebp1c, Acaca, Fasn,* and *Scd1*. The rosiglitazone-dependent transcriptional activity of PPARγ2^{K382Q} was reduced compared with that of PPARγ2^{K382R}. Our findings indicate that SIRT7-dependent PPARγ2 deacetylation at K382 controls lipogenesis in adipocytes.

Methods

Plasmids, antibodies, cell lines, and mice

Detailed information is provided in the supplementary data. The sequences of the primers used to amplify the PPARγ2 mutants and fragments are listed in Supplementary Table S1.

Halo Tag pull-down assay

Halo or Halo-SIRT7 proteins expressed in *Escherichia coli* K12 (KRX; Promega, Madison, WI) were purified with HaloLink resin [14]. The various expression plasmids were transfected into HEK293T cells using the jetPRIME transfection reagent (Polyplus, New York, NY). At 24 h after transfection, the cells were lysed in pull-down buffer (10 mM Tris-HCl [pH 7.4], 1mM NaF, 200 mM NaCl, 10 mM $Na_4P_2O_7$, 1% NP-40, 1 mM PMSF, protease inhibitor cocktail [Nacalai Tesque, Kyoto, Japan]) containing 10 mM nicotinamide (Sigma-Aldrich) and 1 mM TSA (Wako Pure Chemical Industries, Ltd.) by sonication (Sonifier-150; Branson, Cosmo Bio, Carlsbad, CA) at 4°C. Halo or Halo-SIRT7 proteins (30 µg) fixed on HaloLink resin were incubated with HEK293T cell lysate (150 µg) overnight at 4°C, and the resins were washed 5 times with the pull-down buffer. The bound proteins were detected by western blotting with the respective antibody as previously described [9].

Co-immunoprecipitation assay

A co-immunoprecipitation assay was performed as previously described [14]. HEK293T cells transfected with the indicated expression plasmids by the jetPRIME reagent for 24 h were lysed in lysis buffer (20 mM Tris-HCl [pH 7.4], 200 mM NaCl, 2.5 mM $MgCl_2$, 0.5% NP-40, 1 mM PMSF, protease inhibitor cocktail) containing 10 mM nicotinamide and 1 mM TSA by passing through a 29 G needle (Terumo, Tokyo, Japan) 6 times. After centrifugation at 14,000 × *g* for 10 min at 4°C, cell lysate (1,000 µg) was subjected to immunoprecipitation overnight at 4°C with anti-HA antibody beads (clone 4B2; Wako Pure Chemical Industries, Ltd.). To detect interactions between endogenous PPARγ and SIRT7, epididymal WAT (epiWAT) was homogenized with a Dounce homogenizer (Tight; ISIS Co., Ltd., Osaka, Japan) in lysis buffer containing 10 mM nicotinamide and 1 mM TSA on ice. After centrifugation at 14,000 × *g* for 10 min at 4°C, cell lysate (1000 µg) was incubated with anti-PPARγ antibody-crosslinked resin, which was prepared using a Pierce Crosslink Immunoprecipitation Kit (Thermo Scientific, Rockford, IL), at 4°C overnight for immunoprecipitation. After washing 5 times with lysis buffer, precipitated proteins were eluted with the elution buffer (pH 2.8, containing primary amine) provided in the kit, and detected by western blotting with the respective antibody.

Detection of lysine acetylation

HEK293T cells transfected with the indicated plasmids by the jetPRIME reagent for 24 h were lysed in lysis buffer containing 10 mM nicotinamide and 1 µM TSA by sonication (Sonifier-150; Branson) at 4°C. After centrifugation at 14,000 × *g* for 10 min at 4°C, the cell lysates and HA-tag antibody beads (Wako Pure Chemical Industries, Ltd.) were incubated overnight at 4°C. After washing 5 times with lysis buffer, precipitated proteins were eluted with 2× SDS sample buffer (100 mM Tris-HCl [pH 6.8], 4% SDS, 20% glycerol, 0.2% bromophenol blue), and lysine acetylation was detected by western blotting with an anti-acetyl lysine antibody (Cell Signaling Technology). To detect the endogenous acetylation of PPARγ, 350 µg lysate from epiWAT of WT and *Sirt7* KO mice (described above) was incubated with anti-PPARγ antibody-crosslinked resin (described above) at 4°C overnight for immunoprecipitation. Proteins were eluted with the elution buffer provided in the Pierce Crosslink Immunoprecipitation Kit. Acetylation of lysine was detected by western blotting with an anti-acetyl lysine antibody (Cell Signaling Technology).

Retroviral infection and adipocyte differentiation

For knockdown (KD) of *Sirt7*, pSIREN-RetroQ-Sirt7 [12] and pSIREN-RetroQ (negative control) vectors were transfected into Plat-E cells by the jetPRIME reagent. At 48 h after transfection, the retrovirus-containing medium was collected and filtered with a 0.2-µM syringe filter. For PPARγ2 overexpression, pMXs-Puro-PPARγ2-WT, pMXs-Puro-PPARγ2^{K382R}, pMXs-Puro-PPARγ2^{K382Q}, and pMXs (negative control) vectors were used. To generate a stable cell line, C3H10T1/2 cells were infected with these retroviruses for 8 h and selected by treatment with 3 µg/mL puromycin for 72 h. For adipocyte differentiation, at 2 days after reaching confluence, C3H10T1/2 cells were treated with 1 µM dexamethasone (Sigma-Aldrich), 0.5 mM isobutyl-methylxanthine (Sigma-Aldrich), 1.5 µg/mL insulin (Wako Pure Chemical Industries, Ltd.), and 1 µM rosiglitazone (#R2408; Sigma-Aldrich) in maintenance medium for 48 h. Then, the cells were cultured in the maintenance medium with 1.5 µg/mL insulin, which was replenished every 2 days thereafter.

RNA-seq analysis

RNA was extracted using an RNeasy Mini Kit (Qiagen, Hilden, Germany) according to the manufacturer’s instructions. Sequencing libraries were prepared using a NEBNext Ultra II

Directional RNA Library Prep Kit (New England Biolabs, Ipswich, MA) and samples were sequenced on an Illumina NextSeq 500 platform in 76-bp single-end reads. The reads were trimmed for universal Illumina adaptors with TrimGalore (ver 0.6.5) [15] and mapped to transcripts from GENCODE release M25 using salmon (ver 1.2.1) [16] with the default and "GC" parameters. Data were loaded into R using the tximport package (v1.16.0) [17] and aggregated to gene-level abundance in TPM. Differentially expressed genes were determined using DESeq2 (v1.28.0) [18]. Gene ontology analysis was performed using DAVID software [19, 20].

Gene expression analysis

Total RNA was extracted from C3H10T1/2-derived adipocytes and from epiWAT of WT and *Sirt7* KO mice with the Sepasol RNA I Super reagent (Nacalai Tesque). Quantitative real time (qRT)-PCR was performed as previously described [9]. The relative expression of each gene was normalized to that of *Tbp*. Primer sequences are listed in Supplementary Table S2.

Chromatin immunoprecipitation (ChIP) assay

Differentiated C3H10T1/2 cells were fixed in 1% formaldehyde for 5 min at room temperature. Then, the ChIP assay was performed as described in the supplementary data using an anti-PPARγ antibody.

Luciferase assay

HEK293T cells were transfected with pBIND-PPARγ2 LBD^{K382R} or pBIND-PPARγ2 LBD^{K382Q} and pG5luc plasmids using the jetPRIME transfection reagent, followed by treatment with or without 2 μM rosiglitazone. At 18 h after transfection, the cells were lysed and assayed using the firefly and *Renilla* luciferase substrates in the Dual-Luciferase Reporter Assay System (Promega).

Statistical analysis

All results are expressed as the mean ± the standard error of the mean. Statistical significance was determined using the two-tailed Student's *t*-test. A p-value < 0.05 was considered to indicate a significant difference.

Results

SIRT7 interacts with PPARγ2

To investigate the direct regulation of PPARγ2 activity by SIRT7, we first examined whether SIRT7 and PPARγ2 physically interacted with each other. When we performed a Halo tag pull-down assay using lysates from 3×HA-PPARγ2-overexpressing HEK293T cells, Halo-SIRT7, but not Halo, interacted with PPARγ2 (Figure 1a). We also examined the interaction of SIRT7 with PPARγ2 in cultured cells. HEK293T cells were transfected with the 3×HA-PPARγ2 expression plasmid alone or with FLAG-SIRT7, and the resulting cell lysates were immunoprecipitated with anti-FLAG antibody resins. As shown in Figure 1b, PPARγ2 co-immunoprecipitated with SIRT7. The interaction between endogenous PPARγ and SIRT7 was also detected in epiWAT (Figure 1c).

SIRT7 deacetylates PPARγ2

PPARγ is an acetylated protein [8] and SIRT7 is a deacetylase. Thus, we next assessed whether SIRT7 deacetylates PPARγ2. As shown in Figure 2a, PPARγ2 acetylation was detected in HEK293T cells, and SIRT7 overexpression decreased PPARγ2 acetylation, whereas SIRT7^{H188Y} (a loss of function mutant) [9] did not reduce its acetylation. In addition, PPARγ acetylation was increased in epiWAT from *Sirt7* KO mice (Figure 2b). These results indicate that SIRT7 exhibits deacetylation activity for PPARγ2.

SIRT7 deacetylates PPARγ2 at K382

To identify the SIRT7-interacting region of PPARγ2, lysates from HEK293T cells expressing PPARγ2 deletion mutants (GAL4DBD-PPARγ2-M1 [1–200], GAL4DBD-PPARγ2-M2 [201–350], or GAL4DBD-PPARγ2-M3 [351–505]) were pull-downed with Halo or Halo-SIRT7 immobilized resin. As shown in Figure 3a, SIRT7 bound only to GAL4DBD-PPARγ2-M3. Further studies with additional deletion mutants (GAL4DBD-PPARγ2-M3A [351–439] and GAL4DBD-PPARγ2-M3B [440–505]) revealed that SIRT7 specifically bound to the M3A region, which lies in the LBD of PPARγ2 (Figure 3a) [19]. This M3A region contains 6 lysine residues (K364, K382, K386, K395, K401, and K432). To identify the residues targeted by SIRT7, we introduced a deacetylation-mimicking K-to-R mutation into each of the 6 residues and examined the acetylation levels of these mutants in HEK293T cells. As shown in Figure 3b, the acetylation levels of the PPARγ2^{K364R}, PPARγ2^{K395R}, and PPARγ2^{K401R} mutants were similar to those of PPARγ2 WT, whereas the PPARγ2^{K382R}, PPARγ2^{K386R}, and PPARγ2^{K432R} mutants were less acetylated, indicating that K382, K386, and K432 are acetylated in the cells. We next examined whether SIRT7 deacetylates the K382R, K386R, and K432R mutants of PPARγ2. Although SIRT7 reduced the acetylation levels of PPARγ2^{K386R} and PPARγ2^{K432R}, it did not further deacetylate PPARγ2^{K382R} (Figure 3c), indicating that K382 is targeted for deacetylation by SIRT7. This lysine residue is conserved in human, pig, mouse, chicken, frog, and zebrafish and is located in helix 6 of the LBD of PPARγ2 (Figure 3d) [21].

PPARγ2 acetylation at K382 regulates lipid accumulation in adipocytes

Previous studies have shown that SIRT1 attenuates adipogenesis, whereas SIRT7 promotes adipogenesis by inhibiting SIRT1 [7, 13]. We evaluated the role of SIRT7 in mouse mesenchymal C3H10T1/2 cells. Treatment of C3H10T1/2 cells with an adipocytic differentiation cocktail resulted in fat accumulation, as determined by Oil Red-O staining of cellular lipids (Figure 4a). *Sirt7* mRNA levels were significantly increased after day 5 of differentiation (Supplemental Figure 1). Consistent with previous reports [13, 22], *Sirt7* KD led to much less fat accumulation in C3H10T1/2-derived adipocytes after differentiation (Figure 4a). The expression levels of *PPARγ2* and its target genes, such as *Ap2*, *Cd36*, *Adipoq*, and *Lpl*, were significantly decreased in *Sirt7* KD C3H10T1/2-derived adipocytes, but the expression of *Sirt1* mRNA was unchanged (Figure 4b). Then, we investigated the functional roles of PPARγ2 K382 acetylation using these cells. PPARγ2 WT, PPARγ2^{K382R}, and PPARγ2^{K382Q} (acetylation-mimicking mutant) were retrovirally overexpressed in C3H10T1/2 cells and these cells were differentiated into adipocytes. Both PPARγ2 WT- and PPARγ2^{K382R}-expressing cells clearly differentiated into lipid-filled adipocytes, whereas PPARγ2^{K382Q}-expressing cells accumulated less lipid, despite similar PPARγ mRNA expression (Figure 4c and d). Moreover, lipid accumulation was markedly increased by the PPARγ2^{K382R} overexpression in *Sirt7* KD C3H10T1/2-derived adipocytes (Figure 4e). These results indicate that PPARγ2 K382 acetylation affects lipid accumulation in adipocytes. Interestingly, the expression of *Adipoq* and *Lpl* mRNA was lower in PPARγ2^{K382Q}-expressing adipocytes, but the expression levels of other PPARγ2 target genes (*Cebpa* and *Ap2*) were unchanged (Figure 4f), suggesting that the direct effect of SIRT7 on PPARγ2 (K382 deacetylation) is different from the indirect effect (PPARγ2 activation by suppressing SIRT1).

To further investigate the roles of PPARγ2 K382 acetylation in lipid accumulation, we examined global gene expression in PPARγ2^{K382R}- and PPARγ2^{K382Q}-expressing adipocytes by RNA-seq analysis. This analysis revealed that the expression of 469 genes, including *Adipoq* (encoding adiponectin), *Adipsin*, and *Fasn* (encoding fatty acid synthase), was significantly downregulated (fold change > 2) in PPARγ2^{K382Q}-expressing cells compared with that in PPARγ2^{K382R}-expressing adipocytes (Figure 5a). Gene ontology analysis of the downregulated genes in PPARγ2^{K382Q}-expressing cells revealed their significant enrichment in the lipid metabolism process (Figure 5b). qRT-PCR analysis confirmed that the expression levels of a number of genes involved in lipogenesis, such as *Acaca* (encoding acetyl CoA carboxylase α), *Hacd2* (encoding 3-hydroxyacyl CoA dehydratase 2), *Fasn*, *Elovl7* (encoding elongation of very long chain fatty acids-like 7), and *Scd1* (encoding stearoyl CoA desaturase), were significantly lower in PPARγ2^{K382Q}-expressing adipocytes (Figure 5c). Sterol regulatory element-binding protein-1c (SREBP-1c) plays a central role in lipogenesis [23]. The expression of *Srebp1c* mRNA was also lower in PPARγ2^{K382Q}-expressing cells (Figure 5c). PPARγ2^{K382Q} overexpression led to the reduced expression of several PPARγ2 target genes, such as *Adipoq*, *Pck1*, *Adipsin*, and *Lpl*, but it had no effect on the expression of a number of PPARγ2 target genes involved in adipogenesis (such as *Cebpa*, *Cebpb*, *Cebpd*, *Stat5a*, and *Stat5b*) and lipid metabolism (such as *Ap2*, *Acbp*, *Nr1h3*, *Cd36*, and *Acs1*) (Figures 4e, 5c and d). *Sirt1* mRNA expression was also unchanged in PPARγ2^{K382Q}-expressing cells (Figure 5d). Consistently, the expression of lipogenic genes, such as *Fasn*, *Acaca*, and *Srebp1c*, was significantly decreased in epiWAT of *Sirt7* KO mice (Figure 5e).

To understand how K382 acetylation affects gene expression, we compared the binding of PPARγ2^{K382R} and PPARγ2^{K382Q} by a ChIP assay. The binding of PPARγ2^{K382R} and PPARγ2^{K382Q} to the promoter of the *Adipsin* and *Lpl* genes was similar (Figure 5f), suggesting that K382 acetylation does not affect the DNA-binding ability of PPARγ2. We next investigated the influence of K382 acetylation on the ligand-dependent activity of PPARγ2. HEK293T cells were transfected with an expression vector containing the PPARγ2 LBD fused with the GAL4 DBD and a luciferase reporter plasmid driven by GAL4 binding sites. The transcriptional activity of PPARγ2^{K382Q} induced by rosiglitazone was significantly reduced by as much as 40% compared with that of PPARγ2^{K382R} (Figure 5g), indicating that K382 acetylation alters ligand-dependent PPARγ2 activity.

Discussion

Lysine acetylation is a well-known post-translational modification that affects the function of a variety of proteins [24]. PPARγ is an acetylated protein, and SIRT1-dependent deacetylation at K268 and K293 modulates PPARγ coactivator/corepressor exchange [8]. In the present study, we found that SIRT7 deacetylates PPARγ2 at K382 and enhances fat accumulation in adipocytes by regulating the expression of genes involved in lipogenesis (Figure 6). SIRT1 is activated upon fasting and promotes fat mobilization [7]. Thus, SIRT1 and SIRT7 exert clearly opposite roles in lipid accumulation. It is not presently known how the functions of SIRT1 and SIRT7 are integrated *in vivo*, but SIRT7 may be suppressed in a low-energy state, as reported previously [25].

The mechanism by which K382 acetylation controls lipid accumulation in adipocytes is unclear, but we found that the ligand-dependent transcriptional activity of PPARγ2^{K382Q} was reduced. K382 is located within the helix 6 region of the LBD, which forms the ligand-binding pocket of PPARγ2 [21, 26]. Ligand binding or co-regulator recruitment may be differentially regulated by K382 acetylation. More studies are needed to clarify the functional roles of PPARγ2 K382 acetylation.

SREBP-1c plays an important role in lipogenesis [23]. We showed that the expression levels of *Srebp1c* and its target genes, including *Acaca*, *Fasn*, and *Scd1*, were significantly lower in PPARγ2^{K382Q}-expressing cells than in PPARγ2^{K382R}-expressing cells. *Srebp1c* transcription is regulated by liver X receptor α (LXRα), and *Nr1h3* (encoding LXRα) is a target gene of PPARγ2 [27]. However, the expression of *Nr1h3* mRNA was unchanged in PPARγ2^{K382Q}-expressing cells. Thus, it is unlikely that PPARγ2^{K382Q} regulates *Srebp1c* mRNA expression through the regulation of *Nr1h3*. Further studies are necessary to elucidate the mechanism.

Recent studies clarified that post-translational modifications regulate the function of PPARγ2 [1, 3]. For example, phosphorylation of S273 in PPARγ2 alters the transcription of a distinct group of genes whose expression is altered in obesity, and non-thiazolidinedione compounds that block PPARγ2 phosphorylation at S273 exhibit excellent anti-diabetic effects [28, 29]. Our findings suggest that low molecular weight compounds inhibiting the deacetylation of K382 in PPARγ2 may have a beneficial effect against metabolic syndrome and/or type 2 diabetes by decreasing the accumulation of fat in adipocytes.

In conclusion, we clarified that SIRT7 controls lipogenesis and lipid metabolism in adipocytes by directly regulating the acetylation of PPARγ2. Our findings may have significant implications for the development of novel drugs against obesity and type 2 diabetes.

Acknowledgments

This study was supported by a Grant-in-Aid for Scientific Research (B) (19H03711; K.Y., 20H04107; T.Y.), Challenging Research (Exploratory) (19K22639; K.Y.), and Scientific Research on Innovative Areas "LipoQuality" (18H04676; T.Y.) from MEXT, Japan; by a grant from the Japan Agency for Medical Research and Development under Grant Number (JP20gm5010002; K.Y.); and by grants from the Naito Foundation (K.Y.) and Takeda Science Foundation (K.Y., T.Y.).

Disclosure

The authors declare no conflicts of interest associated with this manuscript.

References

1. Ahmadian M, Suh JM, Hah N, *et al.* PPARγ signaling and metabolism: the good, the bad and the future. *Nat Med* 2013; 19: 557-566.
2. Rangwala SM, Lazar MA. Peroxisome proliferator-activated receptor γ in diabetes and metabolism. *Trends Pharmacol Sci* 2004; 25: 331-336.
3. Sauer S. Ligands for the nuclear peroxisome proliferator-activated receptor gamma. *Trends Pharmacol Sci* 2015; 36: 688-704.
4. Soccio RE, Chen ER, Lazar MA. Thiazolidinediones and the promise of insulin sensitization in type 2 diabetes. *Cell Metab* 2014; 20: 573-591.
5. Houtkooper RH, Pirinen E, Auwerx J. Sirtuins as regulators of metabolism and healthspan. *Nat Rev Mol cell biol* 2012; 13: 225-238.
6. Yamagata K, Yoshizawa T. Transcriptional regulation of metabolism by SIRT1 and SIRT7. *Int Rev Cell Mol Biol* 2018; 335:143-166.
7. Picard F, Kurtev M, Chung N, *et al.* Sirt1 promotes fat mobilization in white adipocytes by repressing PPAR-γ. *Nature* 2004; 429: 771-776.
8. Qiang L, Wang L, Kon N, *et al.* Brown remodeling of white adipose tissue by SirT1-dependent deacetylation of Pparγ. *Cell* 2012; 150: 620-632.
9. Yoshizawa T, Karim MF, Sato Y, *et al.* SIRT7 controls hepatic lipid metabolism by regulating the ubiquitin-proteasome pathway. *Cell Metab* 2014; 19: 712-721.
10. Karim MF, Yoshizawa T, Sobuz SU, *et al.* Sirtuin 7-dependent deacetylation of DDB1 regulates the expression of nuclear receptor TR4. *Biochem Biophys Res Commun* 2017; 490: 423-428.
11. Ryu D, Jo YS, Sasso GL, *et al.* A SIRT7-dependent acetylation switch of GABPβ1 controls mitochondrial function. *Cell Metab* 2014; 20: 856-869.
12. Fukuda M, Yoshizawa T, Karim MF, *et al.* SIRT7 has a critical role in bone formation by regulating lysine acylation of SP7/Osterix. *Nat Commun* 2018; 9: 1-14.

13. Fang J, Ianni A, Smolka C, *et al.* Sirt7 promotes adipogenesis in the mouse by inhibiting autocatalytic activation of Sirt1. *PNAS* 2017; 114: E8352-E8361.
14. Sobuz SU, Sato Y, Yoshizawa T, *et al.* SIRT7 regulates the nuclear export of NF-κB p65 by deacetylating Ran. *Biochim Biophy Acta Mol Cell Res* 2019; 1866: 1355-1367.
15. http://www.bioinformatics.babraham.ac.uk/projects/trim_galore/.
16. Patro R, Duggal G, Love MI, *et al.* Salmon provides fast and bias-aware quantification of transcript expression. *Nat Methods* 2017; 14: 417-419.
17. Soneson C, Love MI, Robinson MD. Differential analyses for RNA-seq: transcript-level estimates improve gene-level inferences. *F1000* 2015; 4.
18. Love MI, Huber W, Anders S. Moderated estimation of fold change and dispersion for RNA-seq data with DESeq2. *Genome Biol* 2014; 15: 550.
19. Huang DW, Sherman BT, Lempicki RA. Bioinformatics enrichment tools: paths toward the comprehensive functional analysis of large gene lists. *Nucleic Acids Res* 2009; 37: 1-13.
20. Sherman BT, Lempicki RA. Systematic and integrative analysis of large gene lists using DAVID bioinformatics resources. *Nat Protoc* 2009; 4: 44.
21. Chandra V, Huang P, Hamuro Y, *et al.* Structure of the intact PPAR-γ–RXR-α nuclear receptor complex on DNA. *Nature* 2008; 456: 350-356.
22. Cioffi M, Vallespinos-Serrano M, Trabulo SM, *et al.* MiR-93 controls adiposity via inhibition of Sirt7 and Tbx3. *Cell Rep* 2015; 12: 1594-1605.
23. Shao W, Espenshade PJ. Expanding roles for SREBP in metabolism. *Cell Metab* 2012; 16: 414-419.
24. Choudhary C, Weinert BT, Nishida Y, *et al.* The growing landscape of lysine acetylation links metabolism and cell signalling. *Nat Rev Mol cell biol* 2014; 15: 536-550.

25. Chen S, Seiler J, Santiago-Reichelt M, *et al.* Repression of RNA polymerase I upon stress is caused by inhibition of RNA-dependent deacetylation of PAF53 by SIRT7. *Mol Cell* 2013; 52: 303-313.

26. Shang J, Brust R, Mosure SA, *et al.* Cooperative cobinding of synthetic and natural ligands to the nuclear receptor PPARγ. *Elife* 2018; 7: e43320.

27. Seo JB, Moon HM, Kim WS, *et al.* Activated liver X receptors stimulate adipocyte differentiation through induction of peroxisome proliferator-activated receptor γ expression. *Mol Cell Biol* 2004; 24: 3430-3444.

28. Choi JH, Banks AS, Estall JL, *et al.* Anti-diabetic drugs inhibit obesity-linked phosphorylation of PPARγ by Cdk5. *Nature* 2010; 466: 451-456.

29. Choi JH, Banks AS, Kamenecka TM, *et al.* Antidiabetic actions of a non-agonist PPARγ ligand blocking Cdk5-mediated phosphorylation. *Nature* 2011; 477: 477-481.

Supporting information

Supplementary Methods (Plasmids, antibodies, cell lines and mice)

(Oil Red-O staining)

(Chromatin immunoprecipitation (ChIP) assay)

Supplementary Table S1 (Primer sequences used for plasmid construction)

Supplementary Table S2 (Primer sequences used for qRT-PCR)

Figure legends

Figure 1. SIRT7 interacts with PPARγ2. (a) Halo-SIRT7 pull-down assay was performed using lysates from 3×HA-PPARγ2-overexpressing HEK293T cells to detect the binding between PPARγ2 and SIRT7. **(b, c)** Co-immunoprecipitation assay between FLAG-SIRT7 and 3×HA-PPARγ2 in HEK293T cells (**b**) and between endogenous SIRT7 and PPARγ in epiWAT (**c**).

Figure 2. SIRT7 deacetylates PPARγ2. (a) Effect of SIRT7 overexpression on the acetylation of the PPARγ2 mutants. HEK293T cells were transfected with the 3×HA-PPARγ2 and PCAF expression plasmids, as well as FLAG-SIRT7 or FLAG-SIRT7^{H188Y}. The acetylation level of PPARγ2 was determined by immunoprecipitation and western blotting analysis. **(b)** Effect of SIRT7 deficiency on the endogenous acetylation of PPARγ. Protein lysates of epiWAT from WT and *Sirt7* KO mice were subjected to immunoprecipitation, after which acetylated PPARγ was detected by western blotting analysis.

Figure 3. K382 is a target of the SIRT7-mediated deacetylation of PPARγ2. (a) Mapping of SIRT7-interacting sites in PPARγ2 by a pull-down assay. Schematic diagrams of GAL4DBD-fused mouse deletion mutants of PPARγ2, namely, M1 (1–200), M2 (201–350), M3 (351–505), M3A (351–439), and M3B (440–505), are illustrated on the left side. Halo-

SIRT7-FLAG pull-down assay with lysates from HEK293T cells expressing the indicated PPARγ2 deletion mutants fused with GAL4DBD (right). **(b)** Acetylation of KR mutants of PPARγ2. HEK293T cells were transfected with the indicated 3×HA-PPARγ2 expression vectors. PPARγ2 acetylation was examined by immunoprecipitation and western blot analysis. **(c)** Effect of SIRT7 on the acetylation of the PPARγ2 KR mutants. HEK293T cells were transfected with PCAF and the indicated expression plasmids. PPARγ2 acetylation was examined by immunoprecipitation and western blot analysis. **(d)** Alignment of the PPARγ2 LBD from different species. The K382 of mouse PPARγ2 (red) is highly conserved in the indicated vertebrates.

Figure 4. PPARγ2 acetylation at K382 regulates lipid accumulation. (a) Effect of *Sirt7* KD on Oil Red-O staining in adipocytes. C3H10T1/2 cells were infected with control and *Sirt7* short hairpin RNA retrovirus. After selection by puromycin, C3H10T1/2 cells were differentiated into adipocytes for 5 days. Representative images of 3 independent experiments are shown. **(b)** Gene expression of *Sirt1*, *Sirt7*, *Pparg2*, and target genes for PPARγ2 in differentiated C3H10T1/2 adipocytes (n = 3). **(c, d)** Effect of PPARγ2 WT, PPARγ2^{K382R}, and PPARγ2^{K382Q} overexpression on Oil Red-O staining in adipocytes. C3H10T1/2 cells were infected with control retrovirus or retroviruses expressing PPARγ2, PPARγ2^{K382R}, and PPARγ2^{K382Q}. After puromycin selection, the cells were differentiated into adipocytes for 5 days. Representative images (**c**) and expression of *Pparg2* mRNA (**d**) from 3 independent experiments are shown. **(e)** Effect of PPARγ2^{K382R} overexpression on Oil Red-O staining in adipocytes. Control and *Sirt7* KD-C3H10T1/2 cells were infected with retroviruses expressing PPARγ2^{K382R}, and the cells were differentiated into adipocytes for 5 days. **(f)** Expression of PPARγ2 target genes in differentiated C3H10T1/2-derived adipocytes expressing PPARγ2^{K382R} and PPARγ2^{K382Q} (n = 3). Data are shown as the mean ± the standard error of the mean. $*p < 0.05$.

Figure 5. PPARγ2 acetylation at K382 regulates the expression of lipogenesis-related genes. (a) Volcano plot derived from RNA-seq analysis of PPARγ2^{K382R}- and PPARγ2^{K382Q}-expressing adipocytes. Transcripts downregulated (fold change > 2, $p < 0.05$) in PPARγ2^{K382Q}-expressing adipocytes are in blue. **(b)** Gene ontology analysis of the downregulated genes in PPARγ2^{K382Q}-expressing cells. **(c, d)** Expression of genes involved in lipid metabolism (**c**) and adipocyte differentiation (**d**) in PPARγ2^{K382R}- and PPARγ2^{K382Q}-expressing adipocytes (n = 3). **(e)** Expression of lipogenic genes in epiWAT of WT and *Sirt7* KO mice (n = 4). **(f)** ChIP for the recruitment of PPARγ to the indicated genes in PPARγ2^{K382R}- and PPARγ2^{K382Q}-expressing adipocytes (n = 3). Quantification of enrichment is represented as fold-enrichment relative to IgG. **(g)** Effect of K382 acetylation on the ligand-dependent activity of PPARγ2 in HEK293T cells. The cells were transfected with the GAL4DBD-PPARγ2 LBD^{K382R} or GAL4DBD-PPARγ2 LBD^{K382Q} expression plasmid, as well as the 5×GAL4-luciferase reporter plasmid, followed by treatment with or without rosiglitazone. Luciferase activity was determined after 18 h (n = 4). Data are shown as the mean ± the standard error of the mean. $*p < 0.05$.

Figure 6. Schematic model of SIRT7-mediated deacetylation of PPARγ2.

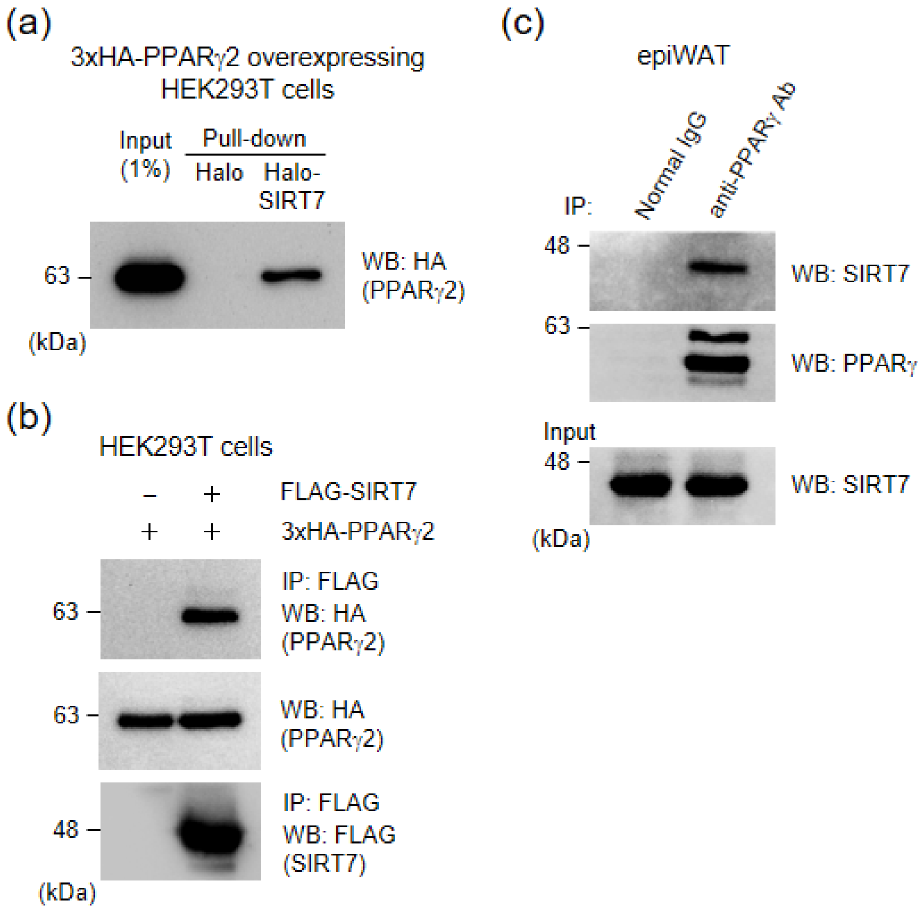
(a)
3xHA-PPARγ2 overexpressing HEK293T cells
Input (1%)
Pull-down
Halo
Halo-SIRT7
63
(kDa)
WB: HA (PPARγ2)
(b)
HEK293T cells
FLAG-SIRT7
3xHA-PPARγ2
63
IP: FLAG
WB: HA (PPARγ2)
63
WB: HA (PPARγ2)
48
IP: FLAG
WB: FLAG (SIRT7)
(kDa)
(c)
epiWAT
IP:
Normal IgG
anti-PPARγ Ab
48
WB: SIRT7
63
WB: PPARγ
Input
48
WB: SIRT7
(kDa)

Figure 1

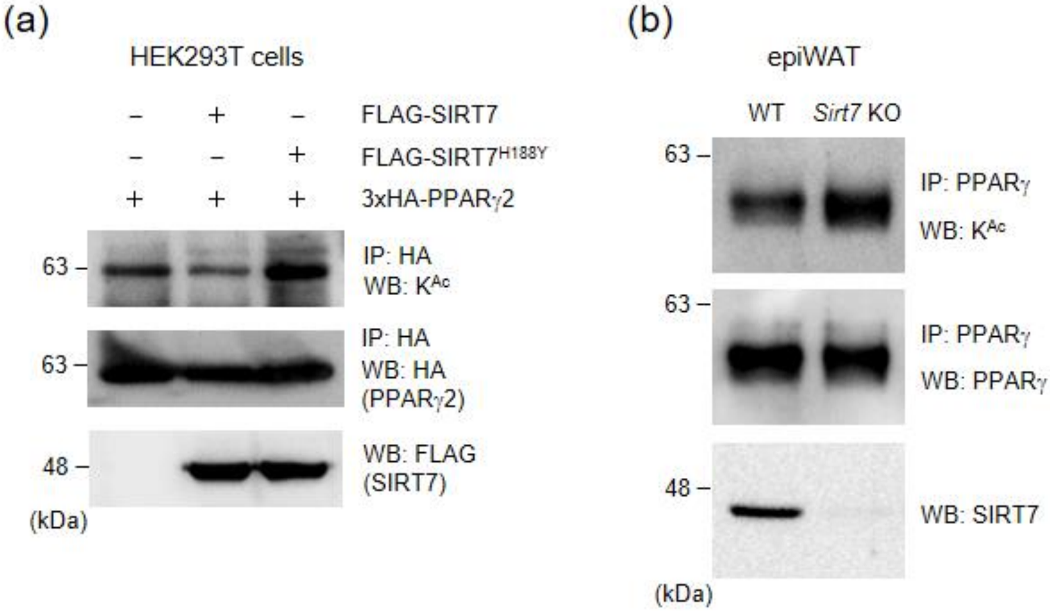
(a)
HEK293T cells
FLAG-SIRT7
FLAG-SIRT7H188Y
3xHA-PPARγ2
63
IP: HA
WB: KAc
63
IP: HA
WB: HA
(PPARγ2)
48
WB: FLAG
(SIRT7)
(kDa)
(b)
epiWAT
WT
Sirt7 KO
63
IP: PPARγ
WB: KAc
63
IP: PPARγ
WB: PPARγ
48
WB: SIRT7
(kDa)

Figure 2

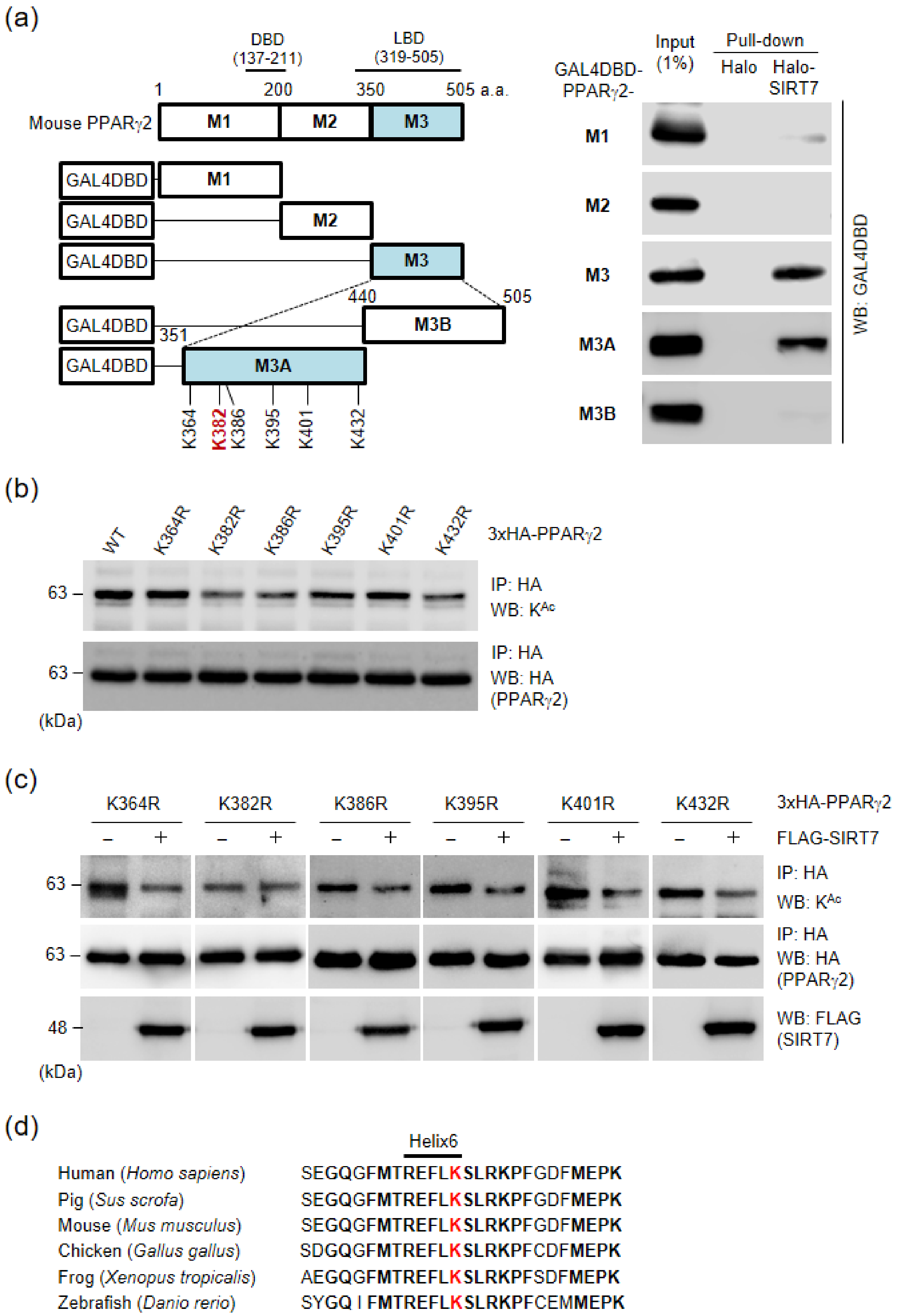
(a)
DBD (137-211)
LBD (319-505)
1
200
350
505 a.a.
Mouse PPARγ2
M1
M2
M3
GAL4DBD
440
505
351
M3B
M3A
K364
K382
K386
K395
K401
K432
GAL4DBD-PPARγ2-
Input (1%)
Pull-down
Halo
Halo-SIRT7
WB: GAL4DBD
(b)
WT
K364R
K382R
K386R
K395R
K401R
K432R
3xHA-PPARγ2
63
IP: HA
WB: K^Ac
WB: HA (PPARγ2)
(kDa)
(c)
FLAG-SIRT7
48
WB: FLAG (SIRT7)
(d)
Helix6
Human (Homo sapiens) SEGQGFMTREFLKSLRKPFGDFMEPK
Pig (Sus scrofa) SEGQGFMTREFLKSLRKPFGDFMEPK
Mouse (Mus musculus) SEGQGFMTREFLKSLRKPFGDFMEPK
Chicken (Gallus gallus) SDGQGFMTREFLKSLRKPFCDFMEPK
Frog (Xenopus tropicalis) AEGQGFMTREFLKSLRKPFSDFMEPK
Zebrafish (Danio rerio) SYGQ I FMTREFLKSLRKPFCEMMEPK

Figure 3

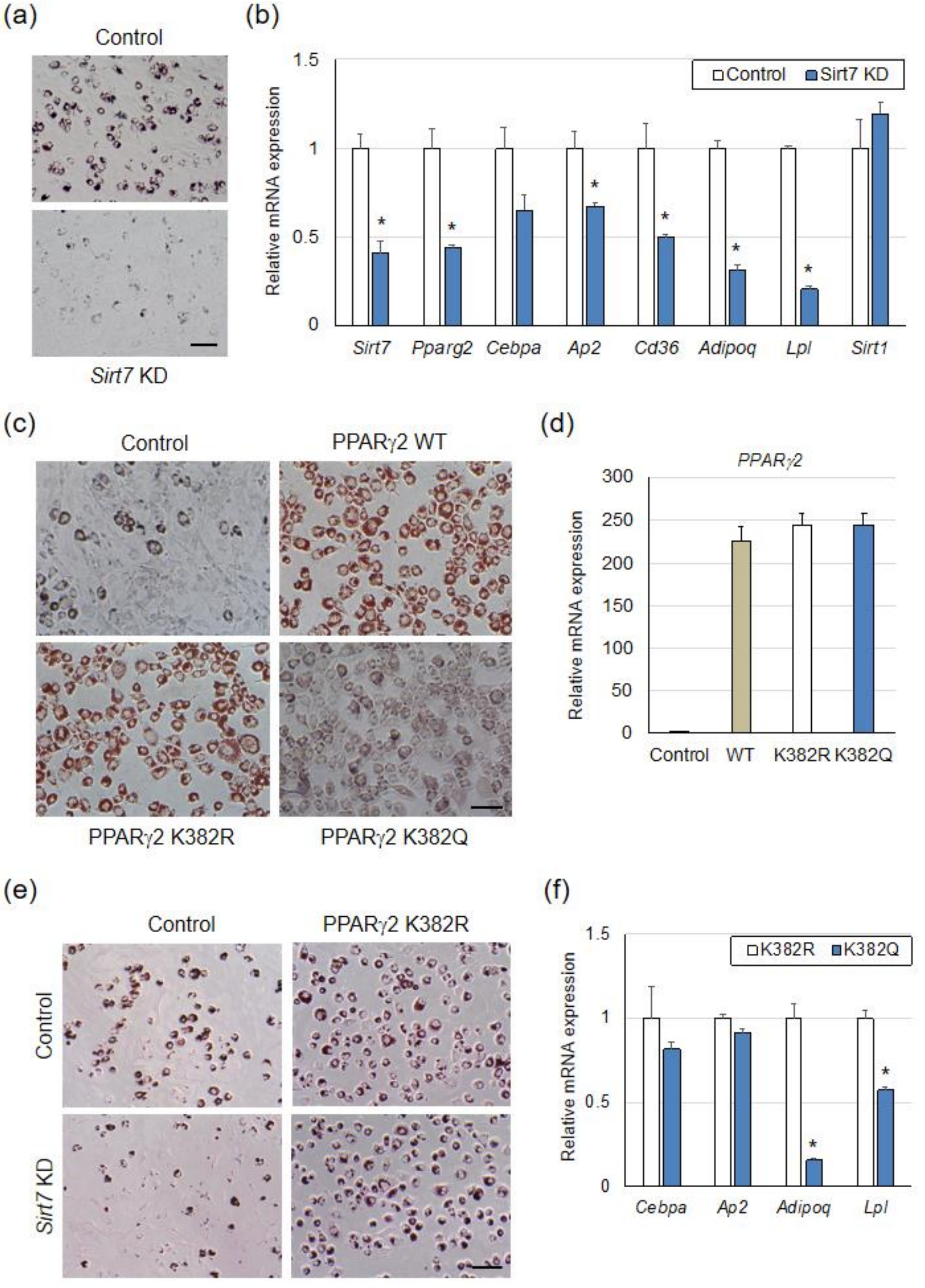
(a)
Control
Sirt7 KD
(b)
□Control ■Sirt7 KD
Relative mRNA expression
1.5
1
0.5
0
*
Sirt7
Pparg2
Cebpa
Ap2
Cd36
Adipoq
Lpl
Sirt1
(c)
Control
PPARγ2 WT
PPARγ2 K382R
PPARγ2 K382Q
(d)
PPARγ2
Relative mRNA expression
300
250
200
150
100
50
0
Control
WT
K382R
K382Q
(e)
Control
PPARγ2 K382R
Control
Sirt7 KD
(f)
□K382R ■K382Q
Relative mRNA expression
1.5
1
0.5
0
*
Cebpa
Ap2
Adipoq
Lpl

Figure 4

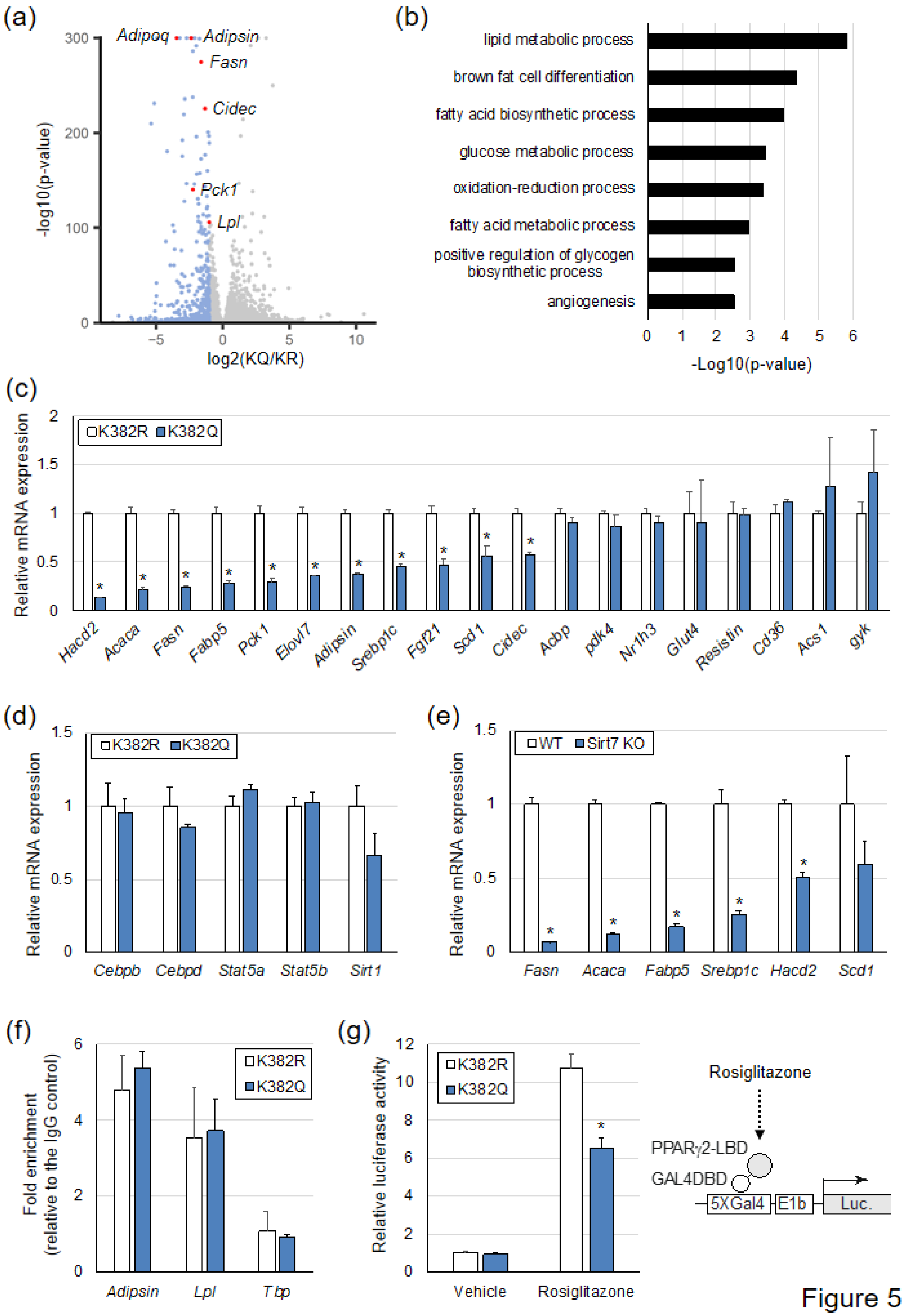
(a)
Adipoq
Adipsin
Fasn
Cidec
Pck1
Lpl
-log10(p-value)
log2(KQ/KR)
300
200
100
0
−5
0
5
10
(b)
lipid metabolic process
brown fat cell differentiation
fatty acid biosynthetic process
glucose metabolic process
oxidation-reduction process
fatty acid metabolic process
positive regulation of glycogen biosynthetic process
angiogenesis
-Log10(p-value)
0
1
2
3
4
5
6
(c)
K382R
K382Q
Relative mRNA expression
2
1.5
1
0.5
0
Hacd2
Acaca
Fasn
Fabp5
Pck1
Elovl7
Adipsin
Srebp1c
Fgf21
Scd1
Cidec
Acbp
pdk4
Nr1h3
Glut4
Resistin
Cd36
Acs1
gyk
(d)
K382R
K382Q
Relative mRNA expression
1.5
1
0.5
0
Cebpb
Cebpd
Stat5a
Stat5b
Sirt1
(e)
WT
Sirt7 KO
Relative mRNA expression
1.5
1
0.5
0
Fasn
Acaca
Fabp5
Srebp1c
Hacd2
Scd1
(f)
Fold enrichment (relative to the IgG control)
K382R
K382Q
6
4
2
0
Adipsin
Lpl
Tbp
(g)
Relative luciferase activity
K382R
K382Q
12
10
8
6
4
2
0
Vehicle
Rosiglitazone
Rosiglitazone
PPARγ2-LBD
GAL4DBD
5XGal4
E1b
Luc.

Figure 5

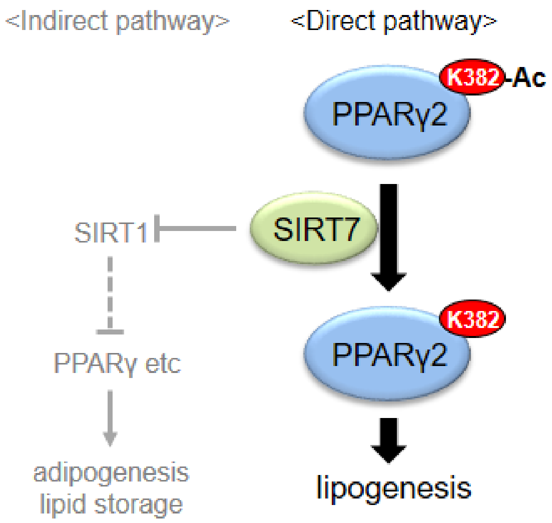
<Indirect pathway>
<Direct pathway>
K382-Ac
PPARγ2
SIRT1
SIRT7
K382
PPARγ2
PPARγ etc
adipogenesis
lipid storage
lipogenesis

Figure 6

SIRT7 regulates lipogenesis in adipocytes through deacetylation of PPARγ2

Fatema Akter[1], Tomonori Tsuyama[2], Tatsuya Yoshizawa[1], Shihab U. Sobuz[1], Kazuya Yamagata[1,2]

[1]Department of Medical Biochemistry, Faculty of Life Sciences, Kumamoto University, Kumamoto 860-8556, Japan

[2]Center for Metabolic Regulation of Healthy Aging (CMHA), Faculty of Life Sciences, Kumamoto University, Kumamoto 860-8556, Japan

Running title: SIRT7 deacetylates PPARγ2

Correspondence to:

Tatsuya Yoshizawa, PhD

Department of Medical Biochemistry,

Faculty of Life Sciences,

Kumamoto University

1-1-1 Honjo, Kumamoto,

Kumamoto 860-8556, Japan

Tel: +81-96-373-5070

Fax: +81-96-364-6940

e-mail: yoshizaw@kumamoto-u.ac.jp

Supplementary data

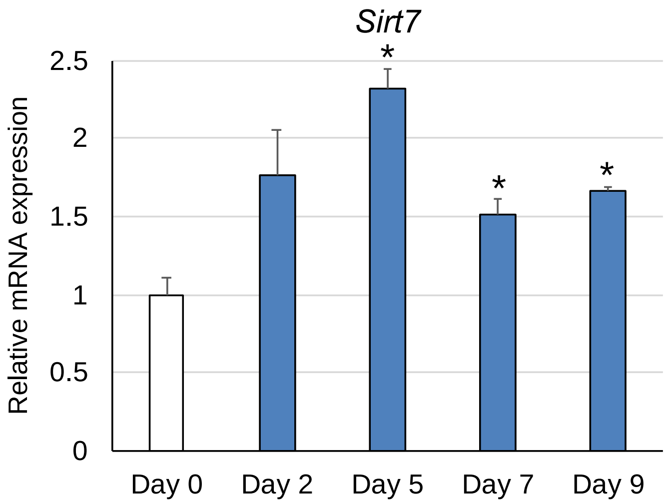

Supplementary Figure 1. The expression of *Sirt7* increases with the differentiation of adipocytes.

Expression of *Sirt7* in C3H10T1/2-derived adipocytes (n = 3). C3H10T1/2 cells were differentiated into adipocytes for 9 days. Data are shown as the mean ± the standard error of the mean. *$p < 0.05$.

Supplementary Methods

Plasmids, antibodies, cell lines, and mice

pcDNA3.1-FLAG-SIRT7, pcDNA3-FLAG-SIRT7^{H188Y}, pFN18A-Halo-SIRT7-FLAG, and pSIREN-RetroQ-Sirt7 were generated as previously described [1, 2]. 5×GAL4-luciferase reporter plasmid (pG5luc), pCl-FLAG-PCAF (#8941), and pSIREN-RetroQ were purchased from Promega, Addgene (Cambridge, MA), and Clontech, respectively. The *Kpn*I/*Nhe*I fragment of pCMX-PPARγ1 [3] was subcloned into pcDNA3.1-3×HA (double-stranded oligo DNA of the HA tag was ligated into pcDNA3) to generate pcDNA3.1-3×HA-PPARγ1. An N-terminal fragment of mouse PPARγ2 was amplified by PCR with primers PPARγ2-F (5′-GGATCCATGGGTGAAACTCTGGGAGATTCT-3′, underlined nucleotides indicate the *Bam*HI cloning site) and PPARγ2-R (5′-AGCAAGGCACTTCTGAAACCGAC-3′) by using mouse WAT cDNA as the template. To generate pcDNA3.1-3×HA-PPARγ2, the *Bam*HI fragment of pcDNA3.1-3×HA-PPARγ1 was replaced with the *Bam*HI fragment of PCR product and verified by sequencing. Various KR and KQ mutants of PPARγ2 were introduced using a KOD-plus Mutagenesis Kit (TOYOBO, Osaka, Japan) and verified by sequencing. For retroviral expression, the N-terminal *Bam*HI fragment and C-terminal *Bam*HI/*Xho*I fragments of pcDNA3.1-3×HA-PPARγ2, pcDNA3.1-3×HA-PPARγ2^{K382R}, and pcDNA3.1-3×HA-PPARγ2^{K382Q} were ligated to the pMXs-Puro retroviral vector. For GAL4DBD fusion PPARγ2 expression, fragments of PPARγ2 (amino acid residues 1-200 [M1], 201-350 [M2], 351-506 [M3], 351-439 [M3A], and 440-506 [M3B]) were amplified by PCR using specific primers, cloned into the pBIND vector (Promega), and verified by sequencing. To generate GAL4DBD fusion PPARγ2 LBD (237-506) expression, PPARγ2 LBD fragments were amplified by PCR using pcDNA3.1-3×HA-PPARγ2^{K382R} and pcDNA3.1-3×HA-PPARγ2^{K382Q} as the template and specific primers, cloned into the pBIND vector, and verified by sequencing. The sequences of the primers used to amplify the PPARγ2 mutants and fragments are listed in Supplementary Table S1.

The primary antibodies used for western blotting were as follows: anti-PPARγ (16643-1-AP; Proteintech Group, Inc, Tokyo, Japan), anti-SIRT7 (clone D3K5A, #5360; Cell Signaling Technology, Danvers, MA), anti-DYKDDDK (FLAG) tag (clone 1E6; Wako Pure Chemical Industries, Ltd., Osaka, Japan), anti-GAL4DBD (G3042; Sigma-Aldrich, St. Louis, MO), anti-HA (clone 3F10; Roche Applied Science, Indianapolis, IN), and anti-acetyl lysine (#9441; Cell Signaling Technology).

HEK293T cells (Clontech, Mountain View, CA) were cultured in Dulbecco's modified Eagle's medium (043-30085; Wako Pure Chemical Industries, Ltd.), with 10% fetal bovine serum (Dominican Republic Origin; Biosera [Wako Pure Chemical Industries, Ltd.]) and 0.1% penicillin/streptomycin. C3H10T1/2 cells (RCB0247), which were provided by the RIKEN BRC through the National Bio-Resource Project of MEXT Japan, were cultured in maintenance medium (Basal Medium Eagle; Gibco BRL, Life Technologies, Carlsbad, CA) supplemented with 10% fetal bovine serum (Dominican Republic Origin; Biosera), 2 mM L-glutamine (GlutaMAX™; Gibco BRL, Life Technologies), and 0.1% penicillin/streptomycin.

This study was approved by the Kumamoto University Ethics Review Committee for Animal Experimentation (A2019-048, A29−001). All mice were housed in a 12-h light/dark cycle and received *ad libitum* access to normal chow and water. Heterozygous *Sirt7*$^{+/-}$ mice [9] were bred, and littermates (WT and *Sirt7* knockout (KO) mice) were used for these studies. All experiments were performed according to the regulations of the Institutional Animal Committee of Kumamoto University.

Oil Red-O staining

C3H10T1/2-derived adipocytes were fixed in 10% formalin at room temperature for 20–30 min. The fixed cells were rinsed with phosphate-buffered saline and incubated with Oil Red-O (O0625; Sigma-Aldrich) solution (0.3% w/v Oil Red-O in 60% isopropanol) for 60 min at room temperature. Before imaging, the cells were washed once with 20% isopropanol and 5 times with phosphate-buffered saline to remove excess stain. Images of the stained cells were taken with a BZ-X700 microscope (Keyence, Osaka, Japan) at 20× optical magnification in phase contrast mode.

Chromatin immunoprecipitation (ChIP) assay

Differentiated C3H10T1/2 cells were fixed in 1% formaldehyde for 5 min at room temperature, and then the reaction was quenched by 150 mM glycine for 5 min. Nuclei isolated in ice cold hypotonic lysis buffer (0.5% Nonidet P-40, 5 mM PIPES, 85 mM KCl) were lysed in SDS lysis buffer (50 mM Tris-HCl (pH 8.0), 1% SDS, 10 mM EDTA). DNA was sheared using Bioruptor sonicator (Diagenode, Denville, NJ) by 15 cycles of sonication at 30 seconds on, 30 seconds off. The sheared chromatin was 5-fold diluted in ChIP dilution buffer (50 mM Tris-HCl (pH 8.0), 167 mMNaCl, 1.1% Triton X-100, and 0.11% sodium deoxycholate), followed by incubation in magnetic beads (Invitrogen Dynabeads protein A and protein G) for one hour at 4°C. After removing the beads, the chromatin was incubated in 4 µg of anti-PPARγ antibody (16643-1-AP; Proteintech), or control IgG (#2729; Cell Signaling Technology) overnight at 4°C. The chromatin was incubated in magnetic beads (Invitrogen Dynabeads protein A and protein G) for 4 h at 4°C, followed by sequential wash with low salt RIPA buffer (50 mM Tris-HCl (pH 8.0), 150 mM NaCl, 1 mM EDTA, 0.1% SDS, 1% Triton X-100, and 0.1%sodium deoxycholate), high salt RIPA buffer (50 mM Tris-HCl (pH 8.0), 500 mM NaCl, 1 mM EDTA, 0.1% SDS, 1% Triton X-100, and 0.1% sodium deoxy-cholate), LiCl wash buffer (10 mM Tris-HCL (pH 8.0), 250 mM LiCl, 1 mM EDTA, 0.5% Nonidet P-40, and 0.5% sodium deoxycholate). The chromatin was eluted and reverse cross-linked in ChIP elution buffer (50 mM Tris-HCl (pH 8.0), 5 mM EDTA, and 0.5% SDS) overnight at 65°C. DNA extraction was performed by Phenol-chloroform extraction and ethanol precipitation. DNA was amplified by qRT-PCR with primers for the *Tbp* gene body (5'-CCCCTTGTACCCTTCACCAAT-3' and 5'-

GAAGCTGCGGTACAATTCCAG-3’), for the *Adipsin* promoter region containing high score of PPARγ-binding in ChIP-Atlas Peak Browser [4] (5’-TACCTTGAGAGTGGGCACTG-3’ and 5’-TCTGCACTTTCGGTGTGTCA-3’), and for the *Lpl* promoter region containing PPRE [5] (5’-CCTCCCGGTAGGCAAACTG-3’ and 5’-AACRGGTGCCAGCGAGAAG-3’).

References

1. Yoshizawa T, Karim MF, Sato Y, *et al.* SIRT7 controls hepatic lipid metabolism by regulating the ubiquitin-proteasome pathway. *Cell Metab* 2014; 19: 712-721.
2. Fukuda M, Yoshizawa T, Karim MF, *et al.* SIRT7 has a critical role in bone formation by regulating lysine acylation of SP7/Osterix. *Nat Commun* 2018; 9: 1-14.
3. Iwaki M, Matsuda M, Maeda N, *et al.* Induction of adiponectin, a fat-derived antidiabetic and antiatherogenic factor, by nuclear receptors. *Diabetes* 2003; 52: 1655-1663.
4. Oki S, Ohta T, Shioi G, *et al.* ChIP-Atlas: a data-mining suite powered by full integration of public ChIP-seq data. *EMBO Rep* 2018; 19: e46255.
5. Helledie T, Grøntved L, Jensen SS, *et al.* The gene encoding the Acyl-CoA-binding protein is activated by peroxisome proliferator-activated receptor gamma through an intronic response element functionally conserved between humans and rodents. *JBC* 2002; 277: 26821-26830.

Supplementary Table S1

Primer sequences used in mutagenesis

Primers	Sequences	
PPARγ2-K364R	Forward	5´CGGGATGGAGTCCTCATCTCA-3´
	Reverse	5´-ATTCATCAGGGAGGCCAGCAT-3´
PPARγ2-K382R	Forward	5´-CGGAGCCTGCGGAAGCCCTTT-3´
	Reverse	5´-GAGGAACTCCCTGGTCATGAA-3´
PPARγ2-K386R	Forward	5´-CGGCCCTTTGGTGACTTTATG-3´
	Reverse	5´-CCGCAGGCTTTTGAGGAACTC-3´
PPARγ2-K395R	Forward	5´-CGGTTTGAGTTTGCTGTGAAG-3´
	Reverse	5´-AGGCTCCATAAAGTCACCAAA-3´
PPARγ2-K401R	Forward	5´-CGGTTCAATGCACTGGAATTA-3´
	Reverse	5´-CACAGCAAACTCAAACTTAGG-3´
PPARγ2-K432R	Forward	5´-CGGCCCATCGAGGACATCCAA-3´
	Reverse	5´-CACGTTCAGCAAGCCTGGGCG-3´
PPARγ2-K382Q	Forward	5´-CAGAGCCTGCGGAAGCCCTTT-3´
	Reverse	5´-GAGGAACTCCCTGGTCATGAA-3´

Primer sequences used in the amplification of PPARγ2 fragments

Primers	Sequences	
PPARγ2-M1	Forward	5´- AATCTAGAGGTGAAACTCTGGGAGA-3´
	Reverse	5´ AAGGTACCCTAAGCAAGGCACTTCTGAAA-3´
PPARγ2-M2	Forward	5´- AATCTAGAGTGGGGATGTCTCACAATGC-3´
	Reverse	5´- AAGGTACCCTAGACACCATACTTGAGCAG-3´
PPARγ2-M3	Forward	5´- AATCTAGACATGAGATCATCTACACG-3´
	Reverse	5´- AAGGTACCCTAATACAAGTCCTTGTAGAT-3´
PPARγ2-M3A	Forward	5´- AATCTAGACATGAGATCATCTACACG-3´
	Reverse	5´- AAGGTACCCTAGTCTTGGATGTCCTCGAT-3´
PPARγ2-M3B	Forward	5´-AATCTAGAAACCTGCTGCAGGCCCTG-3´
	Reverse	5´- AAGGTACCCTAATACAAGTCCTTGTAGAT-3´
The sequences for cloning sites (*XbaI* and *KpnI*) are underlined		
PPARγ2-LBD	Forward	5´-AAGGATCCGTGCTGATCTGCGAGCCCTG-3´
	Reverse	5´-AAGAATTCATGTCGTAGATGACAAAT-3´
The sequences for cloning sites (*Bam*HI and *Eco*RI) are underlined		

Supplementary Table S2

Primer sequences used in quantitative qRT-PCR

Gene	Primer sequences	
Acaca/Acc1	Forward	5´-CCAGCTGATCCTGCGAACCT-3´
	Reverse	5´-GAACATTCCCGCAAGCCATC-3´
Acbp	Forward	5´-AGTCACTTCAAACAAGCTACTG-3´
	Reverse	5´-CACATAGGTCTTCATGGCACT-3´
Acly	Forward	5´-GGCCAGAGAGCTGGGTTTGA-3´
	Reverse	5´-CCCGAGCACAGATGATGGTG-3´
Acs1	Forward	5´-GAACACGAGGCTGTCGCAGA-3´
	Reverse	5´-CTTCCGGAGAACTCGCCTCA-3´
Adiponectin	Forward	5´-CCACCCAAGGGAACTTGTGC-3´
	Reverse	5´-AAGCGGCTTCTCCAGGCTCT-3´.
Adipsin	Forward	5´-GCTATCCCAGAATGCCTCGTT-3´
	Reverse	5´-GGTTCCACTTCTTTGTCCTCGTAT-3´
Ap2	Forward	5´-TCGATGAAATCACCGCAGAC-3´
	Reverse	5´-TGTGGTCGACTTTCCATCCC-3´
Cd36	Forward	5´-TTGGCCAAGCTATTGCGACA-3´
	Reverse	5´-CTGGAGGGGTGATGCAAAGG-3´
Cebpa	Forward	5´-AAGCGGGTGGAACAGCTGAG-3´
	Reverse	5´-AGAGGAAGGGAGGGGACACG-3´
Cebpb	Forward	5´-CAACCTGGAGACGCAGCACAAG-3´
	Reverse	5´-CTAGCAGTGGCCCGCCGAGG-3´
Cebpd	Forward	5´-CGACTTCAGCGCCTACATTGA-3´
	Reverse	5´-CTAGCGACAGACCCCACA-3´
Cidec	Forward	5´-GCGCTTGGCCTTGTAGCAGT-3´
	Reverse	5´-GCTGAAGGGGCAGAAGTGGA-3´.
Elovl6	Forward	5´-GAGCGGCTTCCGAAGTTCAA-3´
	Reverse	5´-GGAGCAGAGGCGCAGAGAAC-3´
Elovl7	Forward	5´-CAGTGTCCCCCAGGTAAGTG-3´
	Reverse	5´-CACAAACCCTACAACCAGTGAC-3´
FabP5	Forward	5´-AATGGGACGGCAAGGAGAGC-3´
	Reverse	5´-GGATGACGAGGAAGCCCTCA-3´.
Fatp1	Forward	5´-GGGAGCCTGACACCCCTCTT-3´
	Reverse	5´-CCCCTGGACACTGGTCCAAC-3´

Fasn	Forward	5′-TCTGGGCCAACCTCATTGGT-3′
	Reverse	5′-GAAGCTGGGGGTCCATTGTG-3′.
Fgf21	Forward	5′-TACACAGATGACGACCAAGA-3′
	Reverse	5′-GGCTTCAGACTGGTACACAT-3′
Glut4	Forward	5′-ACCCCTCATTCCCCCTGTGT-3′
	Reverse	5′-ACCCTCCTGCAGACCCCTTC-3′
Gyk/Gk	Forward	5′-ATCCATGGGGGTGTCCACTG-3′
	Reverse	5′-TTTGTCCCACCAAAGCAGCA-3′
Hacd2	Forward	5′-TGCTATAGGGATTGTGCCATC
	Reverse	5′-ACGGATAATTTCCGTGATTGTCC
Lpl1	Forward	5′- GGGAGTTTGGCTCCAGAGTTT-3′
	Reverse	5′-TGTGTCTTCAGGGGTCCTTAG-3′
Lxrα	Forward	5′-GAGTTGTGGAAGACAGAACCTCAA
	Reverse	5′-GGGCATCCTGGCTTCCTC
Pepck	Forward	5′-TGCGGATCATGACTCGGATG-3′
	Reverse	5′-AGGCCCAGTTGTTGACCAAA-3′.
Pdk4	Forward	5′-CGCGCTCCTGACCCGCAGCC-3′
	Reverse	5′-GCCAGGCGGACGGGCAGCTC-3′
Resistin	Forward	5′-CAGAAGGCACAGCAGTCTTGA-3′
	Reverse	5′-CTGTCCAGTCTATCCTTGCACAC-3′
Tbp	Forward	5′-CCCCTTGTACCCTTCACCAAT-3′
	Reverse	5′-GAAGCTGCGGTACAATTCCA-3′
Scd1	Forward	5′-TGGTTCCCTCCTGCAAGCTC-3′
	Reverse	5′-AATTGTGAGGGTCGGCGTGT-3′.
Sirt1	Forward	5′-TGTGAAGTTACTGCAGGAGTGTA-3′
	Reverse	5′-GCATAGATACCGTCTCTTGATCT-3′
Sirt7	Forward	5′-TGCCAGGCACTTGGTTGTCT-3′
	Reverse	5′-TAGGCTCCGCTTCGCTTAGG-3′
Srebp1c	Forward	5′-ATCGGCGCGGAAGCTGTCGGGGTAGCGTC-3′
	Reverse	5′-ACTGTCTTGGTTGTTGATGAGCTGGAGCAT-3′
Stat5a	Forward	5′-CATTGCTTGGAAGTTTGACTCTC-3′
	Reverse	5′-CACGTAGATAAGGTAGTTCAGGTC-3′
Stat5b	Forward	5′-GCACCTTCAGATCAACCAAA-3′
	Reverse	5′-CAGCTGGGCAAACTGAG-3′